Assessment of the Cold Formability of Ferritic Steels Using Parameters Determined in Uniaxial Tensile Testing

V. Ollilainen

Possibilities and limits of the uniaxial tensile testing in the assessment of cold formability of ferritic low alloy steels are evaluated in the paper. Cold formability covering both sheet and massive forming, including entire formability maps, strain hardening etc., can be estimated from six material parameters determined in a uniaxial tensile test. A master stress strain curve to explain multiple *n* behavior is proposed. Effects of alloying, especially chromium, and other metallurgical parameters on cold formability are discussed.

Keywords

alloying, chromium, formability, forming limit diagram, multiple *n* behavior, steel, tensile test, work hardening

1. Introduction

VARIOUS TECHNOLOGICAL simulation tests (Erichsen test, standardized upsetting test, etc.) have been developed to assess the cold formability in a particular forming method. Since cold formability is influenced not only by the method, but even by specific conditions within the method, the application of simulation leads easily to many different tests (Ref 1).

Another possibility is to correlate cold formability with various material parameters (Ref 1-5). This approach offers a smaller number of tests and good suitability to computer-aided manufacturing and material selection. A reliable assessment of cold formability according to this principle still requires different tests (Ref 4-7).

The uniaxial tensile test, which is a simple, reproducible method available in most material testing laboratories, is often regarded to be capable of measuring only a part of the necessary material parameters. Recent observations with steels, however, show that tensile testing may have more potential than is usually assumed (Ref 8, 9).

This paper deals with possibilities to expand the utility of uniaxial tensile testing in the assessment of cold formability—especially that of ferritic steels—and thus to reduce the number of different test methods needed.

2. Main Aspects of Cold Formability

Flow stress and ductility are often accepted as the main aspects in the concept of cold formability (Ref 10-12). Flow stress is usually expressed as stress-strain relationships and ductility as formability maps (Ref 13).

2.1 *Flow Stress*

Flow stress is characterized by the yield stress of a nondeformed material and the stress-strain relationship in the plastic range.

V. Ollilainen, Imatra Steel, FIN-55100 Imatra, Finland.

2.1.1 Yield Stress

The yield stress of equiaxed, nondeformed ferrite depends on the individual contributions of structural and alloying variables:

$$\sigma_Y = \sigma_Y(\sigma_i, \Delta\sigma_s, \Delta\sigma_p, \Delta\sigma_b)$$

where σ_Y is the lower yield stress; σ_i is the lattice friction; and $\Delta\sigma_s$, $\Delta\sigma_p$, and $\Delta\sigma_b$ are the contributions of solid solutes, particles, and grain boundaries, respectively.

The contribution of the grain boundaries is quantitatively expressed by the Hall-Petch equation (Ref 14-15):

$$\sigma_Y = \sigma_0 + k_y d^{-1/2} \quad \text{(Eq 1)}$$

where σ_0 and k_y are constants and d is grain size. For ferritic steels the Hall-Petch equation is valid over a wide grain-size range, down to 1.6 μm (Ref 16).

Experimentally measured values of the Hall-Petch constants for irons and mild steels with an equiaxed ferritic structure are presented in Table 1, where alloys are divided into three groups:

- *Group I* includes irons and mild steels with a carbon content (x_C) of ≥0.005 wt%. Both constants (σ_0, k_y) have high values.
- *Group II* consists of irons with a maximum carbon content of 0.004 wt%. The constant σ_0 has low values, but k_y is at the same level as in group I.
- *Group III* contains interstitial-free irons, the carbon and nitrogen of which have been removed. Both constants have low values.

As Table 1 shows, the removal of interstitials weakens the contribution of grain boundaries to strength (i.e., reduces k_y), which is related to the change in the locking of dislocations by impurities (Ref 18, 31, 32).

The hardening of an individual solute is approximately proportional to its content, and their effects in ternary alloys are simply additive (Ref 33, 34):

$$\Delta\sigma_s \approx \sum k_i x_i \qquad \text{(Eq 2)}$$

$$\sigma_Y = \sigma_i + \Delta\sigma_s + \Delta\sigma_p + (0 \le k_y \le k_{y_{max}})d^{-1/2} \qquad \text{(Eq 3)}$$

where x_i is the weight percentage of an individual alloying element and k_i is the corresponding solid-solution hardening constant. Experimental k_i values for common solid solutes in ferrite are shown in Table 2.

Chromium causes a weak solid-solution hardening (Table 2), but this is clearly visible in interstitial-free iron alloys only. In commercial steels, chromium interacts with the carbon in ferrite, reducing its solid-solution hardening effect, "cleaning mechanism" (Ref 9, 35). As a result of these contradictory effects, a minimum can be found in the hardening curve by chromium (Fig. 1).

Methods for a quantitative assessment of particle hardening are available in the literature—both for deformable, usually coherent particles and for nondeformable, usually noncoherent particles (e.g., cementite) (Ref 40-42). Elementary hardening contributions are not always directly additive. For instance, grain-boundary hardening is dependent on the presence of nondeformable particles. The yield stress of an alloyed ferrite may be expressed by the applied Hall-Petch equation, which is in the general form (Ref 43):

In alloys with deformable particles, elementary hardening contributions are usually additive, and $k_y = k_{y_{max}}$. In alloys where the strengthening mechanisms interact strongly (Ref 44), such as iron with solid solutes and nondeformable particles, k_y is dependent on $\Delta\sigma_s$ and $\Delta\sigma_p$, and $k_y < k_{y_{max}}$.

For ferritic iron-carbon alloys containing solutes as well as particles, by assuming the values $\sigma_i = 30$ MPa and $k_y = 23$ MPa$\sqrt{\text{mm}}$ (Table 1), the yield stress can be calculated according to the procedure as follows (Ref 9):

- For plain iron-carbon alloys, $\Delta\sigma_s + \Delta\sigma_p = 0$:
- $\sigma_Y = 30 + 23d^{-1/2}$ (Eq 4)
- For iron-carbon alloys with particle hardening caused by deformable (coherent) particles and with a weak solid-solution hardening, $0 < \Delta\sigma_s \le 30$ MPa:

$$\sigma_Y = 30 + \Delta\sigma_s + \Delta\sigma_p + 23d^{-1/2} \qquad \text{(Eq 5)}$$

Table 1 Hall-Petch constants for ferritic irons and steels

Alloy	x_C, wt%	σ_0, MPa	k_y, MPa$\sqrt{\text{mm}}$	Ref
Group I:				
Mild steels and irons with $x_C \ge 0.005$ wt%	0.06	41	20.6	14
	0.02	47	22.4	17
	0.03-0.04	66	23.1	18
	0.04	45	22.5	19
	0.014	63	21.6	20
	0.03	58	15.2	21
	0.05	66	19.6	22
	0.005	73	18.0	23
	0.045	61	21.8	23
	0.046	58	24.3	24
Group II:				
Irons with $x_C \le 0.004$ wt%	0.002	25	23.5	25
	0.004	17	18.4	26
	0.003	25	19.6	27
	0.003	16	16.9	28
Group III:				
Interstitial-free irons	(a)	45	9.7	29
	(b)	36	6.5	29
	(c)	32	5.4	30
	(c)	18	7.6	28
	(d)	32	5.4	30
	(e)	45	5.0	30

(a) Partially decarburized. (b) Decarburized. (c) Iron with 0.15/0.2 wt% Ti. (d) 0.003 wt% C, 1.5 wt% Cr, 0.2 wt% Ti. (e) 0.003 wt% C, 3 wt% Cr, 0.2 wt% Ti

Table 2 k_i and x_i values for ferritic irons and steels

Solute	C	Si	Mn	P	Cr	Ni	Mo	Cu	Sn	Al	N
k_i, MPa/wt%	1.0×10^4	81	18	590	8	8.0	15	40	130	24	2300
$x_{i_{max}}$, wt%	0.013	4	1.5	0.4	12	3	10	1	0.5	8	0.026

Source: Ref 9

- For iron-carbon alloys with a weak particle hardening caused by nondeformable (noncoherent) particles or a weak solid-solution hardening, $0 < \sigma_s + \Delta\sigma_p \leq 30$ MPa, Eq 5 is used.
- For iron-carbon alloys with a substantial amount of solid solution and/or particle hardening caused by nondeformable (noncoherent) particles, $\Delta\sigma_s + \Delta\sigma_p > 30$ MPa, k_y has a linear dependence on σ_0:

$$k_y = 27.1 - 0.068\sigma_0 \quad \text{(Eq 6)}$$

The corresponding yield stress is:

$$\sigma_Y = 30 + \Delta\sigma_s + \Delta\sigma_p + [25.1 - 0.068(\Delta\sigma_s + \Delta\sigma_p)]d^{-1/2} \quad \text{(Eq 7)}$$

which thus is a modified Hall-Petch equation, or a closed form of Eq 3, taking into account the mutual effects of solid-solution, particle, and grain-boundary hardening.

- For interstitial-free alloys:

$$\sigma_Y = 30 + \Delta\sigma_s + \Delta\sigma_p + 5d^{-1/2} \quad \text{(Eq 8)}$$

2.1.2 Stress-Strain Relationship

The yield stress in the plastic range, or flow stress, σ, is affected by numerous variables, such as plastic strain, ε; strain rate, $\dot{\varepsilon}$; temperature, T; and structure:

$$\sigma = \sigma(\varepsilon, \dot{\varepsilon}, T, Y, \ldots) \quad \text{(Eq 9)}$$

where Y represents structural parameters. For practical purposes, one possibility is the use of the mean stress, $\bar{\sigma}$, during forming as a measure of flow stress (Ref 45):

$$\bar{\sigma} = \frac{1}{\varepsilon}\int_0^{\varepsilon} \sigma(\varepsilon)d\varepsilon \quad \text{(Eq 10)}$$

Power Laws. One of the most widely used empirical equations to describe the stress-strain dependence, particularly for steel, is the simple power law (Ref 46):

$$\sigma = K\varepsilon^n \quad \text{(Eq 11)}$$

where K and n are constants. The advantage of the equation is that it contains only two unknown constants: K equal to the stress at unit strain and n to the strain at maximum load in the uniaxial tensile test (Ref 46-48).

The effect of strain rate can be taken into account by adding a power term with strain-rate sensitivity, m:

$$\sigma = K'\varepsilon^{n'}\dot{\varepsilon}^m \quad \text{(Eq 12)}$$

where K′ is a constant. The effect of deformation heating can be expressed by an additional term (Ref 49, 50):

$$\sigma = K'\varepsilon^{n'}\dot{\varepsilon}^m(1 - \beta\Delta T) \quad \text{(Eq 13)}$$

where ΔT is the temperature difference from the isothermal condition and β constant. For steel, $\beta = 0.0015$ 1/K (Ref 49, 50). If the strain rate during deformation is constant, $n = n'$.

For steel, n is the main parameter influencing the strain at maximum load, and other parameters, such as the m value, are of minor importance (Ref 51). A high n value leads to a low strain gradient during forming (e.g., in a neck) (Ref 48).

Even though ferritic steels usually obey the simple power law well, its adequacy is not always perfect. Due to a deviation from linearity for the stress-strain data in a double logarithmic plot, two or three sets of K and n must be used—phenomena that are called double or triple n behavior, respectively. Since the condition for this multiple n behavior is a small Lüder's strain (Ref 52), a masking effect is suggested, in which Lüder's strain masks the initial slope of the stress-strain curve.

For multiple n behavior, the validity ranges of the equations are:

$$\begin{aligned} &\text{I:} \quad \sigma = K_0\varepsilon^{n_0}, \quad \varepsilon_L < \varepsilon \leq \varepsilon_{k0} \\ &\text{II:} \quad \sigma = K_1\varepsilon^{n_1}, \quad \varepsilon_{k0} \leq \varepsilon \leq \varepsilon_{k1} \\ &\text{III:} \quad \sigma = K_2\varepsilon^{n_2}, \quad \varepsilon_{k1} \leq \varepsilon \leq \varepsilon^* \end{aligned} \quad \text{(Eq 14)}$$

where ε_L is the Lüder's strain, ε_{k0} and ε_{k1} are knee strains, and ε^* is strain at maximum load.

Double n behavior is favored by a coarse grain size and by nondeformable particles (Ref 9). The necessary condition for triple n behavior is that $\varepsilon_L < \varepsilon_{k0}$. In ferritic steels, low interstitial content causes a continuous flow curve, making it possible to fulfill this requirement (Ref 9).

A hypothesis has been put forward according to which in uniaxial tension there always exists a master curve of triple n type being more or less masked by ε_L or ε^* (Ref 9). The visible

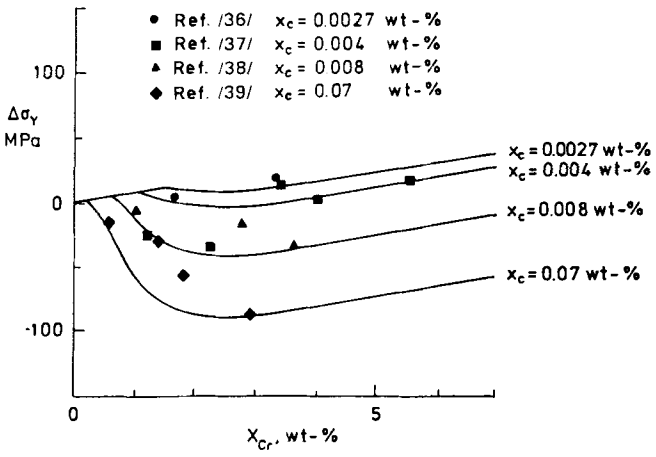

Fig. 1 Effect of chromium on the yield stress of ferritic irons with different carbon contents. The curves are calculated and the dots experimentally determined.

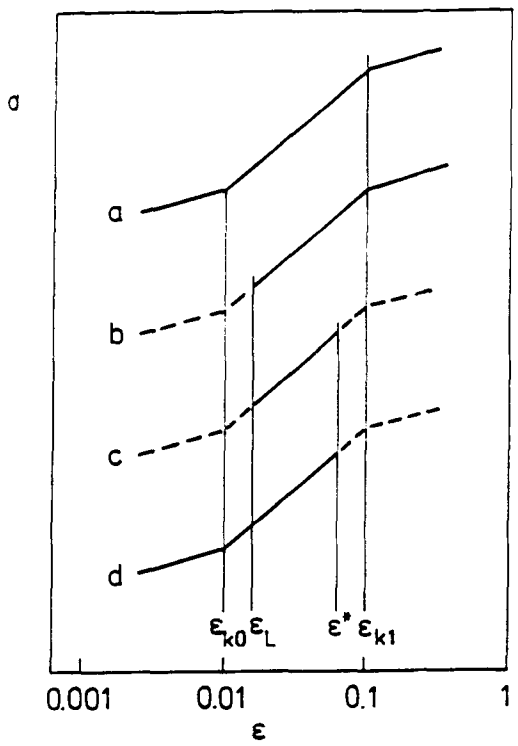

Fig. 2 Hypothetical examples of the masking effects by ε_L and ε^* on the visible stress-strain curve. (a) Triple n master curve. (b) Double n. (c) Single n. (d) Quasi-double n. Source: Ref 9

result may then be triple n, double n, single n, or quasi-double n, depending on the location of the knee strains related to the masking strains (Fig. 2).

When flow stress is determined in the uniaxial tensile test, necking is a restrictive phenomenon. A major limitation in the use of uniaxial tensile testing for the assessment of cold formability of ferritic steels lies in the fact that necking begins already at $\varepsilon \approx 0.2...0.3$. However, there are results showing that beyond the maximum load in tension a simply extrapolated stress-strain curve agrees satisfactorily with the measured curve in compression up to $\varepsilon \approx 1$ (Ref 53-55). Moreover, particular methods have been developed to calculate the flow stress in uniaxial tension up to fracture (Ref 56-58).

The mean flow stress from Eq 9 and 10 is (Ref 59):

$$\bar{\sigma} = \frac{K}{n+1}\varepsilon^n \qquad \text{(Eq 15)}$$

which is up to unity strain:

$$\bar{\sigma}_{\varepsilon=1} = \frac{K}{n+1} \qquad \text{(Eq 16)}$$

indicating K to be a relevant material parameter describing the average flow stress.

Work and Strain Hardening. The term *work hardening* or the *magnitude of work hardening* relates to the increment of stress with the increase of strain (Ref 60-62):

$$\Delta\sigma(\varepsilon) = \sigma(\varepsilon_2) - \sigma(\varepsilon_1) \qquad \text{(Eq 17)}$$

whereas the *rate of work hardening* or *work hardening rate* is the slope of stress-strain curve (Ref 60-62), which according to Eq 9 is:

$$\frac{d\sigma}{d\varepsilon} = \left(\frac{\partial\sigma}{\partial\varepsilon}\right)_{\dot{\varepsilon},T,Y...} + \left(\frac{\partial\sigma}{\partial\dot{\varepsilon}}\right)_{\varepsilon,T,Y...}\left(\frac{d\dot{\varepsilon}}{d\varepsilon}\right) + \left(\frac{\partial\sigma}{\partial T}\right)_{\varepsilon,\dot{\varepsilon},Y...}\left(\frac{dT}{d\varepsilon}\right) + \left(\frac{\partial\sigma}{\partial Y}\right)_{\varepsilon,\dot{\varepsilon},T...}\left(\frac{dY}{d\varepsilon}\right) + ... \qquad \text{(Eq 18)}$$

Equation 18 defines the total rate of work hardening (Ref 60), which is the combined effect of the *rate of strain hardening* (Ref 60, 63):

$$\theta = \left(\frac{\partial\sigma}{\partial\varepsilon}\right)_{\dot{\varepsilon},T,Y...} \qquad \text{(Eq 19)}$$

and the strain-induced secondary processes, such as heating, recovery, and so on, during deformation. The concept of Eq 18 is also the instantaneous rate of work hardening. The *average rate of work hardening* (Ref 60) over a range of strain is defined as:

$$\frac{\Delta\sigma}{\Delta\varepsilon} = \frac{\sigma(\varepsilon_2) - \sigma(\varepsilon_1)}{\varepsilon_2 - \varepsilon_1} \qquad \text{(Eq 20)}$$

The n value is widely called the strain or work-hardening exponent. Cautionary words have been put forward, however, on the use of the n value as a measure of strain or work hardening (Ref 61-66).

From the simple power law, the rate of strain hardening is (Ref 48):

$$\theta - nK\varepsilon^{n-1} = \frac{n\sigma}{\varepsilon} \qquad \text{(Eq 21)}$$

which is at maximum load:

$$\theta_{\varepsilon=n} = Kn^n \approx 0.7K \qquad \text{(Eq 22)}$$

when $n \approx 1/6...1/2$ (Ref 63). The rate of strain hardening at unity strain is

$$\theta_{\varepsilon=1} = Kn \qquad \text{(Eq 23)}$$

Equations 22 and 23 show that K is a valid parameter for strain hardening, but Eq 23 indicates that K and n together are relevant for this purpose, too.

In addition to the definitions in Equations 17 to 20, other ideas related to work hardening have been presented. Hart (Ref 67) defined a function in the state equation:

$$\gamma = \left(\frac{\partial \ln \sigma}{\partial \varepsilon}\right)_{\dot{\varepsilon}} \quad \text{(Eq 24)}$$

which, in other contexts, is called a work-hardening coefficient (Ref 68) or normalized strain hardening, $(1/\sigma)(d\sigma/d\varepsilon)$ (Ref 69). The term *logarithmic* or *incremental work hardening rate*, $d \ln \sigma / d \ln \varepsilon$, being the same as the instantaneous or differential n value, is also used (Ref 68, 70, 71):

$$\frac{d \ln \sigma}{d \ln \varepsilon} = \frac{d\sigma/\sigma}{d\varepsilon/\varepsilon} = n(\varepsilon) \quad \text{(Eq 25)}$$

From Eq 25 it follows that (Ref 68):

$$\gamma = \frac{n(\varepsilon)}{\varepsilon} \quad \text{(Eq 26)}$$

which is at maximum load $\gamma_{\varepsilon=n} = 1$ and at unity strain $\gamma_{\varepsilon=1} = n$. Empirically it has been found that for essentially ferritic steels the alloying elements and a large grain size in solid solution increase the rate of strain hardening (Ref 9, 72).

2.2 *Ductility*

Ductility expresses the ability of a metal to deform plastically. It is usually limited by plastic instability or fracture. For practical forming purposes, the ductility of a particular metal is conveniently described by a formability map.

2.2.1 Plastic Instability

The general Swift-Hill condition for plastic instability (Ref 73, 74) is:

$$\frac{d\sigma_e}{d\varepsilon_e} > \frac{\sigma_e}{Z_x} \quad \text{(Eq 27)}$$

where σ_e is the effective stress, ε_e is the effective plastic strain, and Z_x is the critical subtangent. The value for the critical subtangent at diffuse necking or load maximum in the uniaxial tension of an isotropic material is $Z_d = 1$ (Ref 73, 75). The critical subtangent at localized necking of an anisotropic sheet, Z_l, is defined in Ref 9.

Localized necking, defined by Eq 27, becomes possible only at those stress states where the principal minor strain is negative or zero (Ref 74). For positive principal strains, specific theories for localized necking are suggested. For instance, a localized neck may be initiated from an inhomogeneity in a material according to Marciniak and Kuczynski (M-K theory) (Ref 76) or from a heterogeneous distribution of nonmetallic inclusions (Ref 77).

2.2.2 Fracture

According to the Cockcroft-Latham criterion (Ref 78), ductile fracture occurs when:

$$\int_0^{\varepsilon_f} \sigma_e \left(\frac{\sigma^*}{\sigma_e}\right) d\varepsilon_e = \text{constant} \quad \text{(Eq 28)}$$

where ε_f is the strain at fracture and σ^* is the maximum tensile stress. Based on the process of ductile fracture involving the initiation, growth, and coalescence of voids (Ref 79) and on a statistical process of the shear joining of voids, Ghosh (Ref 80) derived an instantaneous fracture criterion in plane stress:

$$(1 + \alpha)^2 \sigma_1 = K_{CR} \quad \text{(Eq 29)}$$

where K_{CR} is a constant. For porous metals, Oyane (Ref 81) derived a fracture criterion that emphasizes the role of hydrostatic stress, σ_M:

$$\int_0^{\varepsilon_{ef}} \left(1 + \frac{1}{a_0}\frac{\sigma_M}{\sigma_e}\right) d\varepsilon_e = b_0 \quad \text{(Eq 30)}$$

where ε_{ef} is the effective strain at fracture and a_0 and b_0 are constants.

Anisotropy of a metal may be caused by texture, showing variable strengths according to the orientation, or by inhomogeneities, such as nonmetallic inclusions, weakening ductility in some direction. In sheet forming, a high r value (i.e., normal anisotropy coefficient), used as a measure of textural anisotropy, is related with a low susceptibility to fracture in deep drawing (Ref 82).

In massive cold forming (cold forging, bulk cold forming), fracture most often determines formability. In cold upsetting, the fracture strain is influenced by the characteristics of nonmetallic inclusions, such as their size, form, location, and orientation, which affect the initiation of voids (Ref 83-85), and by the tensile hydrostatic stress component promoting the initiation and growth of voids (Ref 83, 85-87).

In cold upsetting, the anisotropy of ductility is significant. Sekiguchi and Osakada (Ref 84) observed that the critical reduction in cold upsetting correlates with the fracture strain in a uniaxial tensile test measured with tensile specimens taken transverse to the rolling direction (Fig. 3). The explanation is the alignment of elongated manganese sulfides causing fracture. On the other hand, in cold extrusion the fracture strain has been shown to be related to axial ductility in a uniaxial tensile test (Ref 88). A characteristic feature of cold upsetting is the change of the hydrostatic stress in the surface of the specimen, which is first negative, but as Fig. 4 shows, in the course of deformation becomes positive and thus able to expand voids.

2.2.3 Prediction of Formability Maps

Formability maps express limits of ductility for a specific material in two-dimensional strain space, displaying information in a form that aids decision-making in material selection and in the design of forming processes. Theoretical predictions

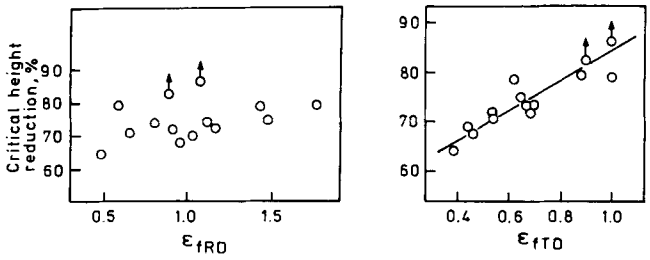

Fig. 3 Critical height reduction in cold upsetting versus axial and transverse fracture strain (ε_{fRD} and ε_{fTD}, respectively) measured in a uniaxial tensile test. Source: Ref 84

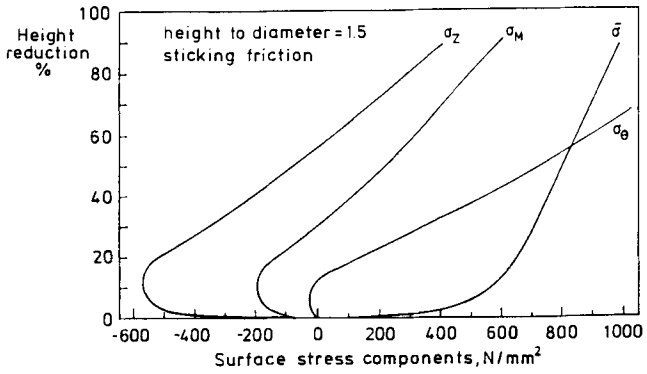

Fig. 4 Change of surface stress components during cold upsetting. Source: Ref 83

of formability maps are still more or less restricted, but they have been complemented by empirical rules (Ref 9).

Formability maps for practical sheet forming, indicating limits at local necking, are usually called forming limit diagrams (FLDs). The terms forming limit diagram at necking (FLDN) and forming limit diagram at fracture (FLDF) can generally be used for sheet as well as bulk forming (Ref 9, 89).

Constructing a complete formability map normally requires different tests. A simpler alternative would be to use only the uniaxial tensile test and then predict the limit curves in other stress states.

Sheet Forming. At negative principal minor strains, an FLDN may be calculated theoretically for an anisotropic material by applying Hill's instability criterion (Eq 28) for an anisotropic material and the simple power law (Ref 9):

$$\varepsilon_{1n} + \varepsilon_{2n} = n \qquad \text{(Eq 31)}$$

where ε_{1n} and ε_{2n} are principal strains at localized necking.

At positive principal strains, a theoretical calculation of FLDN may be carried out from the M-K theories (Ref 76, 90-95). They include an inhomogeneity factor as a material parameter, which cannot easily be assessed. Efforts to use, for example, surface roughness for it have been tried (Ref 94, 95).

An entire FLDN was predicted based on the variation of the density of particles (Ref 77). The fitting parameter in the model could be determined in uniaxial tension, but with ferritic steels the fit was poor at negative minor strains (Ref 53). A recent prediction was attempted based on Hill's nonquadratic yield criterion with a fair agreement for steel (Ref 96, 97).

An empirical procedure has been applied in which forming limit curves for ferritic steels have a constant shape and their intercept with the plane strain axis is determined by the n value (Ref 9, 98). By using uniaxial tensile testing only, a simple possibility is to approximate an entire FLDN from the n value by combining the idea of a constant shape limit curve and the Hill criterion. The limit curve is then calculated from Eq 31 at negative strain ratios and from the parable equation

$$\varepsilon_{1n} = n + \frac{3}{2}\varepsilon_{2n} - \frac{1}{2n}\varepsilon_{2n}^2 \qquad \text{(Eq 32)}$$

at positive strain ratios up to $\rho = 1$ (Ref 9).

A simple way to calculate an FLDF comes from the observation that the thickness fracture strain of steel is approximately independent of stress ratio (Ref 90), which combined with volume constancy leads to a constant thickness criterion (Ref 99):

$$\varepsilon_{1f} + \varepsilon_{2f} = \text{constant} \qquad \text{(Eq 33)}$$

where ε_{1f} and ε_{2f} are principal strains at fracture.

Ghosh (Ref 80) derived from Eq 29 strains at fracture for materials with normal anisotropy. By measuring fracture strains in the uniaxial tension, he determined K_{CR} and then predicted the FLDF (Ref 9, 80). An attempt to simplify Ghosh's method was made by measuring only the longitudinal strain in the uniaxial tensile test and assuming a fixed strain ratio, $\rho = -1/2$ (Ref 100). Both procedures gave an equal agreement with empirical results in the case of aluminium-killed steel, but for niobium-alloy steel the original one was better. Ghosh's method was also modified by assuming a linear strain path between the limit strain at localized necking and fracture at negative minor strains, achieving for a ferritic chromium steel an agreement as good as that of the original method (Ref 101).

From the Latham-Cockcroft criterion, Jalinier (Ref 89) derived the following fracture condition:

$$P' = \frac{K}{\sqrt{1 - \alpha_1 + \alpha_1^2}} \int_0^{\varepsilon_{en}} \varepsilon_e^n d\varepsilon_e + \frac{K}{\sqrt{1 - \alpha_2 + \alpha_2^2}} \int_{\varepsilon_{en}}^{\varepsilon_{ef}} \varepsilon_e^n d\varepsilon_e \qquad \text{(Eq 34)}$$

where P' is a constant, ε_{en} is the effective strain at localized necking, α_1 is the stress ratio before localized necking, and α_2 is the stress ratio after that. Based on the fracture condition in Eq 34, Jalinier described a method in which the limit curve can be calculated by determining the fracture strain in one stress state. When this method is modified by introducing the normal anisotropy according to Hill's model (Ref 102), the principal strains at fracture are obtained as follows:

$$\varepsilon_{1f} = \left[\frac{\sqrt{3}\,P'(n+1)}{2KD'^{n+1}} - \varepsilon_{1n}^{n+1}\left(\frac{\sqrt{3}}{2C'} - 1\right)\right]^{1/(n+1)} \qquad \text{(Eq 35a)}$$

$$\varepsilon_{2f} = \varepsilon_{2n} \quad \text{(Eq 35b)}$$

where

$$C' = \left[3\frac{(1+r)\alpha^2 - 2r\alpha + (1+r)}{2(2+r)}\right]^{1/2} \quad \text{(Eq 35c)}$$

$$D' = \frac{1}{(1+r-r\alpha)}\left\{\frac{2}{3}(2+r)[(1+r)\alpha^2 - 2r\alpha + (1+r)]\right\}^{1/2} \quad \text{(Eq 35d)}$$

where

$$\alpha = [(1+r)\rho + r]/(1+r+r\rho) \text{ (Levy Mises)} \quad \text{(Eq 35e)}$$

The constant P′ is determined from the equation:

$$P' = D'^{n+1}_U \frac{K}{n+1}\left[\left(\frac{1}{C'_U} - \frac{2}{\sqrt{3}}\right)\varepsilon^{n+1}_{1n} + \frac{2}{\sqrt{3}}\varepsilon^{n+1}_{1fU}\right] \quad \text{(Eq 36)}$$

in which C'_U and D'_U are received from Eq 35c and 35d by using the strains measured in a uniaxial tensile test (ε_{1fU}, ε_{2fU}). The limit strains at localized necking are calculated from Eq 31 and 32. Different from Ghosh's method, the strain ratio here is $\rho = \varepsilon_{2n}/\varepsilon_{1n}$ due to the verticality of the second strain path.

Figure 5 shows that predicted FLDNs calculated from Eq 31 and 32 agree satisfactorily with the measured values. Similarly, in the prediction of FLDF the methods used—that of Ghosh (Ref 9, 80), the modified method of Jalinier (Eq 35 and 36), and the constant thickness criterion (Eq 33)—give satisfactory agreement. On the whole, formability maps are predicted for ferritic sheet steels from the parameters determined in a uniaxial tensile test, including the effect of differences in the alignment of nonmetallic inclusions (RD and TD curves) and in the steel matrix interstitial and grain size/strength levels (Ref 9).

Massive Forming. In cold upsetting, the FLDF is usually presented in a plot with axial strain against tangential strain. When the fracturing mode is longitudinal cracking, the FLDF most often assumes the form of a straight line with a slope of approximately $^{-1}/_{2}$ being most common for ferritic steels (Ref 54, 85, 103-106). Lahti et al. (Ref 85, 104) observed that test conditions determined the strain path in upsetting and expressed the tangential strain as a function of axial strain, which made it possible to use Oyane's criterion. By determining the constants a_0 and b_0 in different test conditions, a good agreement with the calculated and experimental FLDF was achieved (Ref 85).

The fracture strain in cold upsetting may also be predicted from uniaxial tensile testing according to the correlation in Fig. 3. The main factors influencing fracture strain are the characteristics of the second-phase particles, particularly nonmetallic inclusions, and the tensile hydrostatic stress affecting the initiation and growth of voids. By using a transverse tensile test specimen, the effect of nonmetallic inclusions elongated in the rolling direction, such as manganese sulfides, can be taken into account. In fact, the procedure includes the consequence of hydrostatic stress since during the deformation this becomes positive (Fig. 4). Calculations with ferritic steels in sticking friction conditions show that the hydrostatic stress becomes positive at tangential strains of $\varepsilon_\theta \approx 0.1...0.3$ (Ref 103, 107). Particularly at a height-to-diameter ratio of 1.5, used in a standardized cold upsetting test (Ref 108), $\varepsilon_\theta \approx 0.2$ (Ref 103, 107), which is far below normal fracture strains. The final process, including void growth, takes place under a tensile hydrostatic stress in both tests, confirming the findings by Sekiguchi and Osakada (Fig. 3).

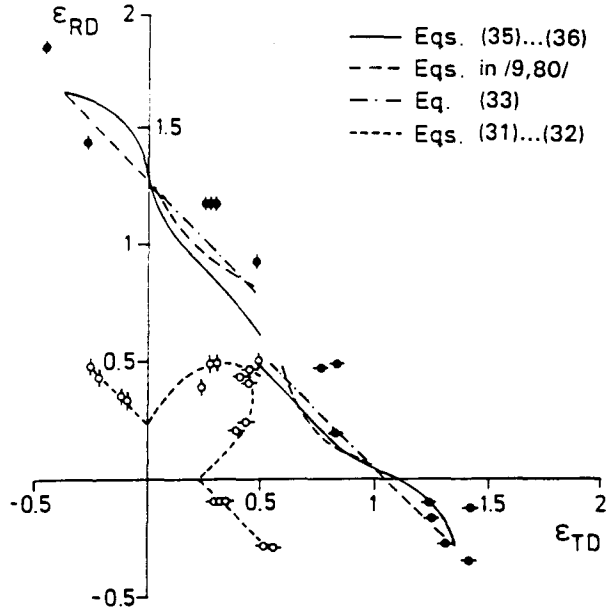

Fig. 5 Predicted and measured formability map for a ferritic, low-carbon, 4% Cr-Nb steel. Source: Ref 9

One upsetting condition is sufficient for an estimation of an FLDF for ferritic steels, when the slope of $^{-1}/_{2}$ is applied. A more trustworthy prediction, however, requires two tests in different conditions to enable the determination of both constants in Oyane's criterion and, in this way, the calculation of the limit curve with the method described above (Ref 85).

3. Assessment of Cold Formability

Although cold formability of the workpiece material can be evaluated to a great extent by the main aspects of flow stress and ductility, this is only a rough simplification. Kudo (Ref 11) described a cold-forming system including sequential operations, such as workpiece material selection; billet preparation; cold forming and subsequent operations; hardware, such as the workpiece, lubricant, tooling, and press; and software for these. In a broad sense, cold formability should cover all of these system components.

Marciniak et al. (Ref 1, 4, 5) have systematically approached the concept of cold formability. Phenomena that limit cold formability can be divided into those limiting the maximum deformation and those making the quality of the product unsatisfactory. (Ref 1). Furthermore, cold formability involves both intrinsic material properties, tied in with the internal struc-

ture of the material, and extrinsic ones, such as dimensional accuracy and freedom from defects (Ref 1, 109).

In this paper the concept of cold formability will be restricted by considering it only as an intrinsic material property limiting the maximum deformation.

3.1 *Criteria for Cold Formability*

When the cold formability of a specific material is evaluated, the forming method and the criterion of formability must be defined (Ref 1). Marciniak (Ref 1, 110), Devendzic (Ref 111), and Dodd (Ref 112) have outlined the phenomena limiting cold formability. Of those, the following limit cold formability in the restricted sense described above:

- Damage of tools
- Failure of the workpiece outside the forming region
- Fracture of the workpiece; brittle or ductile fracture
- Localized necking
- Wrinkling or puckering
- Undesirable changes in physical properties

In one operation there may be different possible limiting phenomena. The phenomenon that occurs first is regarded as the criterion of cold formability (Ref 1).

In sheet forming, failure of the workpiece outside the forming region may be the limiting phenomenon in deep drawing (Ref 1). Fracture of the workpiece may limit formability in such operations as stretching, deep drawing, and bending (Ref 1, 6, 96, 113). In deep drawing in particular, examples are splits in the corners of rectangular cups and other components, where high strain gradients occur (Ref 99). Localized necking may be the limiting phenomenon in stretching and bending, while wrinkling may be that in deep drawing and bending (Ref 1, 6).

In massive forming, damage of tools may be the limiting phenomenon in closed-die extrusion, hobbing, heading, and inner upsetting (Ref 1, 4, 5). Failure outside the forming region is often the limiting phenomenon in open-die extrusion, ironing, bar drawing, and expanding, whereas fracture of the workpiece may restrict forming in upsetting, sleeve upsetting, bending, expanding, heading, and edge curling (Ref 1, 4, 5, 114).

Table 3 Testing methods and "standard" material parameters suggested for the assessment of cold formability in sheet forming

Testing method	Material parameter
Uniaxial tensile test	Yield strength, R_e
	Tensile strength, R_m
	Flow stress
	n or n' value
	Uniform elongation, e_U
	r value
	Minimum normal anisotropy, r_{min}
	Thickness reduction at fracture
Uniaxial and biaxial tensile test	Ratio of uniaxial to biaxial flow stress
Biaxial tensile test	Limit strain at localized necking, ε_{1n}

Source: Ref 1, 2, 70

3.2 *Testing for Cold Formability*

As stated earlier, the principle of correlating cold formability with material parameters has wide possibilities, offering an approach with a limited number of tests and suitability to computer-aided manufacturing and material selection. For the assessment of our restricted concept of cold formability, Marciniak (Ref 1) suggested the following basic material features:

- Proneness to brittle fracture
- Yield stress level (K in $\sigma = K\varepsilon^n\dot{\varepsilon}^m$)
- Strain-hardening index (n)
- Strain-rate sensitivity (m)
- Fracture strain (ε_f)
- Normal anisotropy coefficient (r)
- Inhomogeneity coefficient (M-K theory)
- Elastic energy stored

Instead of the basic features, standard material parameters are also applied for assessing formability. For sheet operations, both uniaxial and biaxial tensile tests are then needed (Table 3). Massive forming often requires more tests (Table 4). Marciniak et al. (Ref 1, 4, 5) created a system in which standard material parameters are linked with the forming operation through the limiting phenomenon. This principle enables the calculation of the possibility of forming a workpiece, the determination of the critical value of a forming parameter, and the specification of the necessary material properties. From the parameters presented in Table 4, the method includes six necessary ones: R_e, Z, $\sigma_{0.6}$, ε_0, n, and S, thus requiring three different tests.

3.3 *Utility of Uniaxial Tensile Testing*

For the creation and updating of computer-aided material selection systems, it is important that the stored material properties, such as cold formability, be defined by parameters that are relevant, comparable, and easily measurable. The parameters determined using uniaxial tensile testing offer, in this respect, a simple possibility. To assess the above-defined cold formability, material characteristics and the related material parameters measurable in a uniaxial tensile test are suggested

Table 4 Testing methods and "standard" material parameters suggested for the assessment of cold formability in massive forming

Testing method	Material parameter
Hardness test	Vickers hardness, HV
	Brinell hardness, HB
Uniaxial tensile test	Yield strength, R_e
	Tensile strength, R_m
	Uniform elongation, e_U
	Reduction of area, Z
Uniaxial frictionless compression test	Flow stress at the strain 0.6 or 1, $\sigma_{0.6}$ or σ_1, n or n'
Upsetting test	Upsettability ratio, S, or critical height reduction

Source: Ref 1, 4, 5, 11, 88, 114, 115

in Table 5 (ε_{fRD} and ε_{fTD} are strains at fracture measured in the rolling and transverse directions, respectively).

The parameters in Table 5 have a true nature compared with the standard ones (e.g., σ_T versus R_m, etc.), being well suited for material data banks. Their measurement is easy with computerized material testing, and they require only one test method instead of the two tests usually needed for sheet forming and three or four for massive forming (Tables 3 and 4).

In the present suggestion, σ_T or K and n are parameters for flow stress and work hardening. These can be used to predict the flow stress in static cold-forming processes, where the effects of strain rate and deformation heating are not decisive. Particularly when an exact numerical value of flow stress is not needed, the uniaxial tensile test can be used with a sufficient accuracy for the formability rating of different metals.

Even though with ferritic steels the simply extrapolated stress-strain curve in tension seems to agree satisfactorily with the measured curve in compression (Ref 53-55), and even though methods have been developed to calculate the flow stress in uniaxial tension up to fracture (Ref 56-58) (section 2.1.2), very large strains ($\varepsilon >> 1$) must be considered outside the capability of the uniaxial tensile test (Ref 116).

In dynamic processes with very high strain rates, the estimation of flow stress is more complex. In systematic experimental studies on dynamic cold upsetting of ferritic steels, Tozawa (Ref 117) found a plateau in the flow stress curves from a strain of $\varepsilon \approx 0.4$ due to adiabatic heating. In tests with different steels and variable strain rates, the intercept of the static and dynamic flow curve was also practically constant ($\varepsilon \approx 0.7...0.8$). An exact prediction of the dynamic flow stress could be made, based on the state equations complemented by the low-temperature effects of strain rate (Ref 118).

Strain at localized necking (FLDN) for ferritic steels is governed by the n value with an accuracy necessary for practical forming purposes (Ref 9, 98). The total FLDF in sheet forming can be determined from ε_f measured in a uniaxial tensile test by applying the method of Ghosh (Ref 80) or the modified one of Jalinier (Ref 89). In massive forming, ε_{fRD}, determined using a uniaxial tensile test, may be utilized in forming methods where the reduction of area in a uniaxial tensile test is critical—for example, in bending, expanding, and forward extrusion (Ref 5). Accordingly, ε_{fTD}, ascertained in a uniaxial tensile test, can be employed to predict the critical reduction in upsetting operations.

To sum up, using the parameters in Table 5, uniaxial tensile testing can be applied for the assessment of cold formability covering both sheet and massive forming. The major limitations or difficulties exist in the prediction of flow stress, particularly at very large strains ($\varepsilon >> 1$) and in dynamic processes at very high strain rates.

Table 5 Material parameters for the assessment of cold formability using uniaxial tensile testing only

Main aspect	Material characteristic	Material parameter
Flow stress	Yield stress	σ_Y
	Flow stress	K (or σ_T)
	Work hardening	K and n
Ductility	Strain at localized necking	n (or ε^*)
	Strain at fracture	ε_{fRD} and ε_{fTD}
	Plastic anisotropy	r

4. Conclusions

When cold formability is considered as an intrinsic material property of ferritic steels covering both sheet and massive forming, it can be assessed using uniaxial tensile testing from the following six material parameters: σ_Y, K, n, ε_{fRD}, ε_{fTD}, and r. Major limitations exist in the accurate prediction of flow stress, particularly at very large strains ($\varepsilon >> 1$) and in dynamic forming processes at very high strain rates.

An entire formability map for ferritic sheet steels is predictable from parameters determined in a uniaxial tensile test. An FLDN for ferritic steels is approximated from the n value, and an FLDF using the methods of Ghosh and Jalinier.

An FLDF in cold upsetting of ferritic steels may be roughly predicted from uniaxial tensile testing when using transverse test specimens. The effect of nonmetallic inclusions elongated in the rolling direction and of hydrostatic stress are then taken into account, since the final fracturing process, including void growth, takes place under a tensile hydrostatic stress in both tests.

Valid parameters for prediction of strain hardening are K or K and n together.

In uniaxial tension it is possible that there always exists a master curve of triple n type being more or less masked by ε_L or ε^*. The visible result may then be triple n, double n, single n, or quasi-double n, depending on the location of the knee strains related to the masking strains.

For iron-carbon alloys with a substantial amount of solid solution and/or particle hardening caused by nondeformable particles, a modified Hall-Petch equation can be applied, where k_y has a linear dependence on σ_0, taking into account the mutual effects of solid-solution, particle, and grain-boundary hardening.

Acknowledgment

The author would like to thank Dr. Bradley Dodd for his advice and helpful discussions.

References

1. Z. Marciniak, in *Advanced Technology of Plasticity,* Japan Society for Technology of Plasticity, Tokyo, 1984, p 685-694
2. R.D. Butler, *Sheet Metal Ind.,* Vol 41, 1964, p 705-716
3. H. Kudo, K. Sato, K. Aoi, and I. Sawano, *J. Jpn. Soc. Technol. Plast.,* Vol 9, 1968, p 569-578
4. Z. Marciniak and A. Turno, "Assessment of the Material Formability in Cold Forging Operations," presented at 14th Plenary Meeting of ICFG, Birmingham, UK, 1981
5. *Computer Aided Engineering—Metal Forming Processes, Part One, User's Manual,* Technical University of Warsaw, Warsaw, 1986
6. J. Kumpulainen, D. Tech. thesis, Helsinki University of Technology, Espoo, Finland, 1984
7. M.P. Miles, J.L. Siles, R.H. Wagoner, and K. Narasimhan, *Metall. Trans. A,* Vol 24A, 1993, p 1143-1151

8. H. Sekiguchi and K. Osakada, *Ann. CIRP,* Vol 32, 1983, p 181-185
9. V. Ollilainen, D. Tech thesis, Helsinki University of Technology, Espoo, Finland, 1988
10. V. Ollilainen and M. Sulonen, *Belch Rohre Profile,* Vol 25, 1978, p 403-409
11. H. Kudo, in *25th Int. Machine Tool Design and Research Conf.,* S.A. Tobias, Ed., MacMillan, London, 1985, p 49-61
12. J. Havranek, *Met. Australas.,* Nov/Dec 1984, p 9-11
13. J.D. Embury and J.L. Duncan, *Ann. Rev. Mater. Sci.,* Vol 11, 1981, p 505-521
14. E.O. Hall, *Proc. Phys. Soc. B,* Vol 64, 1951, p 747-753
15. N.J. Petch, *J. Iron Steel Inst.,* Vol 174, 1953, p 25-28
16. E.P. Abrahamson, in *Surfaces and Interfaces,* Vol II, J.J. Burke, N.L. Read, and V. Weiss, Ed., Syracuse University Press, 1968, p 262-269
17. A. Cracknell and N.J. Petch, *Acta Metall.,* Vol 3, 1955, p 186-189
18. J. Heslop and N.J. Petch, *Philos. Mag.,* Vol 2, 1957, p 649-658
19. D.V. Wilson and B. Russell, *Acta Metall.,* Vol 8, 1960, p 36-45
20. H. Conrad and G. Schoeck, *Acta Metall.,* Vol 8, 1960, p 791-796
21. M.M. Hutchison, *Philos. Mag.,* Vol 8, 1963, p 121-127
22. W.B. Morrison, *Trans. ASM,* Vol 59, 1966, p 824-846
23. D.V. Wilson, *Met. Sci. J.,* Vol 1, 1967, p 40-47
24. K.D. Sibley and N.N. Breyer, *Metall. Trans. A,* Vol 7A, 1976, p 1602-1604
25. B.W. Christ and G.V. Smith, *Acta Metall.,* Vol 15, 1967, p 809-816
26. D.J. Dingley and D. McLean, *Acta Metall.,* Vol 15, 1967, p 885-901
27. W. Roberts and Y. Bergström, *Z. Metallkd.,* Vol 62, 1971, p 752-757
28. I.M. Bernstein and B.B. Rath, *Metall. Trans.,* Vol 4, 1973, p 1545-1551
29. R. Armstrong, I. Codd, R.M. Douthwaite, and N.J. Petch, *Philos. Mag.,* Vol 7, 1962, p 45-58
30. W.B. Morrison and W.C. Leslie, *Metall. Trans.,* Vol 4, 1973, p 379-381
31. I. Codd and N.J. Petch, *Philos. Mag.,* Vol 5, 1960, p 30-42
32. J.C.M. Li, *Trans. AIME,* Vol 227, 1963, p 239-247
33. F.B. Pickering and T. Gladman, *ISI Spec. Rep.,* Vol 81, 1963, p 10-20
34. C.E. Lacy and M. Gensamer, *Trans. ASM,* Vol 32, 1944, p 88-110
35. J.R. Low, Jr., Discussion in *Trans. ASM,* Vol 31, 1943, p 336-337
36. J.L. Englehard, J.K. O'Donnell, P.R. Mould, and G.V. Smith, *J. Iron Steel Inst.,* Vol 207, 1969, p 371-373
37. W.P. Rees, B.E. Hopkins, and H.R. Tipler, *J. Iron Steel Inst.,* Vol 177, 1954, p 93-110
38. E. Anderson and J. Spreadborough, *J. Iron Steel Inst.,* Vol 206, 1968, p 1223-1235
39. T. Matsuoka and K. Yamamori, *Metall. Trans. A,* Vol 6A, 1975, p 1613-1622
40. E. Orowan, Discussion in *Symp. Internal Stresses in Metals and Alloys,* Institute of Metals, London, 1948, p 451-453
41. M.F. Ashby, in *Oxide Dispersion Strengthening,* G.S. Ansell, Ed., TMS-AIME, 1958, p 143-212
42. U.F. Kocks, A.S. Argon, and M.F. Ashby, *Progress in Materials Science,* Vol 19, Pergamon Press, Oxford, 1975
43. E. Hornbogen, in *Strength of Metals and Alloys* (ICSMA 5), Vol 2, P. Haasen, V. Gerald, and G. Kostorz, Ed., Pergamon, Oxford, 1979, p 1337-1342
44. H. Martikka, H. Eskelinen, and R. Suoranta, *Proc. 4th Finnish Mech. Days,* Lappeenranta, 1991, p 243-252
45. P. Huml, Contribution to ICFG Materials and Defects Subgroup, Osaka, 1989
46. J.R. Low, Jr. and T.A. Prater, "Final Report on Plastic Flow of Aluminium Aircraft Steel under Combined Loads—II," OSRD No. 4052, Pennsylvania State College, 1944
47. J.H. Hollomon, *Trans. AIME,* Vol 162, 1945, p 268-290
48. M. Gensamer, *Trans. ASM,* Vol 36, 1946, p 30-60
49. A.S. Korhonen and H.J. Kleemola, *Metall. Trans. A,* Vol 9A, 1978, p 979-986
50. H.J. Kleemola and A.J. Ranta-Eskola, *Sheet Metal Ind.,* Vol 56, 1979, p 1046-1057
51. K. Chung and R.H. Wagoner, *Metall. Trans. A,* Vol 19A, 1988, p 293-300
52. W. Dahl and H. Rees, *Arch. Eisenhüttenwes.,* Vol 50, 1979, p 401-406
53. A. Melander, E. Schedin, S. Karlsson, and J. Steninger, *Scand. J. Metall.,* Vol 14, 1985, p 127-148
54. K. Olsson, S. Karlsson, and A. Melander, *Scand. J. Metall.,* Vol 15, 1986, p 283-256
55. D.N. Johnson and F. Ebrahimi, in *Near Net Shape Manufacturing,* P.W. Lee and B.L. Ferguson, Ed., ASM International, 1988, p 245-251
56. G. Lange, *Arch. Eisenhüttenwes.,* Vol 45, 1974, p 809-812
57. K. Saka, M.J. Painter, and R. Pearce, *J. Mech. Work. Technol.,* Vol 3, 1979, p 17-30
58. R.A. Ayres, *Metall. Trans. A,* Vol 14A, 1983, p 2269-2275
59. B. Dodd, Reading University, private communication, 1991
60. G.W. Geil and N.L. Carwile, *J. Res. NBS,* Vol 45, 1950, p 129-147
61. R.E. Reed-Hill, *Rev. High-Temp. Mater.,* Vol 1, 1972, p 99-154
62. A.W. Bowen and P.G. Partridge, *J. Phys. D, Appl. Phys.,* Vol 7, 1974, p 969-978
63. U.F. Kocks, *STP 765,* ASTM, 1982, p 121-138
64. D.V. Wilson, *J. Phys. D, Appl. Phys.,* Vol 7, 1974, p 954-968
65. W. Dahl, W. Hesse, A. Krabiell, and H.J. Rosezin, *Nucl. Eng. Des.,* Vol 76, 1983, p 309-318
66. G.V. Smith, *Cold Working of Metals,* American Society for Metals, 1949, p 2-30
67. E.W. Hart, *Acta Metall.,* Vol 18, 1970, p 599-610
68. L. Ratke and P.I. Welsh, "Efficiency in Sheet Metal Forming," IDDRG 13th Biennial Congress, Melbourne, 1984, p 427-435
69. J.E. Bird and J.L. Duncan, *Metall. Trans. A,* Vol 12A, 1981, p 235-241
70. K. Yoshida, K. Yoshii, H. Komorida, and M. Usuda, *Sheet Metal Ind.,* Vol 48, 1971, p 772-791
71. R.H. Wagoner, *Metall. Trans. A,* Vol 12A, 1981, p 877-882
72. T. Gladman, B. Holmes, and F.B. Pickering, *J. Iron Steel Inst.,* Vol 208, 1970, p 172-183
73. H.W. Swift, *J. Mech. Phys. Solids,* Vol 1, 1952, p 1-18
74. R. Hill, *J. Mech. Phys. Solids,* Vol 1, 1952, p 19-30
75. G.G. Moore and J.F. Wallace, *J. Inst. Met.,* Vol 93, 1964, p 33-38
76. Z. Marciniak and K. Kuczynski, *Int. J. Mech. Sci.,* Vol 9, 1967, p 609-620
77. A. Melander, *Mater. Sci. Eng.,* Vol 58, 1983, p 63-88
78. M.G. Cockcroft and D.J. Latham, NEL Report No. 240, 1966
79. F.A. McClintock, *J. Appl. Mech.,* Vol 35, 1968, p 363-368
80. A.K. Ghosh, *Metall. Trans. A,* Vol 7A, 1976, p 523-533
81. M. Oyane, *Bull. JSME,* Vol 15, 1972, p 1507-1513
82. W.T. Lankford, S.C. Snyder, and J.A. Bauscher, *Trans. ASM,* Vol 42, 1950, p 1197-1232
83. I. Lahti and M. Sulonen, *Scand. J. Metall.,* Vol 11, 1982, p 9-16
84. H. Sekiguchi and K. Osakada, *Ann. CIRP,* Vol 32, 1983, p 181-185
85. S. Kivivuori, I. Lahti, and V. Ollilainen, in *Computational Methods for Predicting Material Processing Defects,* M. Predeleanu, Ed., Elsevier, Amsterdam, 1987

86. H. Sekiguchi and K. Osakada, in *Advanced Technology of Plasticity,* Japan Society for Technology of Plasticity, Tokyo, 1984, p 851-856
87. B. Dodd and Y. Bai, *Ductile Fracture and Ductility,* Academic Press, London, 1987
88. T. Miki, T. Tamano, and S. Yanagimoto, in *Proc. 6th North American Metalworking Research Conf.,* 1978, p 185-192
89. J.M. Jalinier, *J. Mater. Sci.,* Vol 18, 1983, p 1794-1802
90. Z. Marciniak, K. Kuczynski, and T. Pokora, *Int. J. Mech. Sci.,* Vol 15, 1973, p 789-805
91. A.K. Tandros and P.B. Mellor, *Int. J. Mech. Sci.,* Vol 17, 1975, p 203-210
92. R.D. Venter and G. Kharshafdjian, in *Process Modeling—Fundamentals and Applications to Metals,* American Society for Metals, 1978, p 275-285
93. K.W. Neale and E. Chater, *Int. J. Mech. Sci.,* Vol 22, 1980, p 563-574
94. K. Yamaguchi, S. Nishimura, N. Takakura, and M. Fukuda, in *4th Int. Conf. on Production Engineering,* Japan Society of Precision Engineering, Tokyo, 1980, p 155-160
95. J.Z. Gronostajski and Z. Zimniak, *J. Mater. Process. Technol.,* Vol 32, 1992, p 263-270
96. R. Hill, *Math. Proc. Camb. Philos. Soc.,* Vol 85, 1979, p 179-191
97. H. Pishbin and P.P. Gillis, *Metall. Trans. A,* Vol 23A, 1992, p 2817-2831
98. S.P. Keeler and W.G. Brazier, in *Micro Alloying 75,* Union Carbide, 1977, p 517-530
99. A.G. Atkins, "The Mechanics of Ductile Fracture in Metalforming," presented at 13th Plenary Meeting of ICFG, Paris, 1980
100. J. Tmej and K. Dadourek, *Strojírenství,* Vol 28, 1978, p 298-301
101. V. Ollilainen, in *4th Int. Conf. Production Engineering,* Japan Society of Precision Engineering, Tokyo, 1980, p 711-718
102. R. Hill, *The Mathematical Theory of Plasticity,* Clarendon Press, Oxford, 1950
103. S. Kivivuori and M. Sulonen, *Ann. CIRP,* Vol 27, 1978, p 141-145
104. I. Lahti and M. Sulonen, *Scand. J. Metall.,* Vol 11, 1982, p 9-16
105. P.W. Lee and H.A. Kuhn, *Metall. Trans.,* Vol 4, 1973, p 969-974
106. N.L. Dung and O. Mahrenholz, in *Advanced Technology of Plasticity 1987,* K. Lange, Ed., Springer, Berlin, 1987, p 1013-1020
107. I. Lahti, Lic. Tech. thesis, Helsinki University of Technology, Espoo, Finland, 1983
108. B. de Meester and Y. Tozawa, *Ann. CIRP,* Vol 28, 1979, p 577-580
109. K. Yoshida and K. Miyauchi, in *Mechanics of Sheet Metal Forming: Material Behaviour and Deformation Analysis,* D.P. Koistinen and N.-M. Wong, Ed., Plenum Press, 1978, p 19-52
110. Z. Marciniak, Contribution to ICFG Materials and Defects Subgroup, Osaka, 1993
111. B. Devendzic, in *Proc. 26th Int. Mach. Tool Design and Research Conf.,* B.J. Davies, Ed., Macmillan, 1986, p 443-451
112. B. Dodd, "Defects in Cold Forging," Final Report by the Materials and Defects Subgroup of the ICFG, Osaka, 1993
113. S.K. Ghosh, *Int. J. Mech. Sci.,* Vol 23, 1981, p 195-211
114. H. Kudo, K. Sato, and K. Aoi, *Ann. CIRP,* Vol 16, 1968, p 309-318
115. H. Wozniak and A. Turno, Metal Forming Institute Papers, Poznan, 1987
116. M.G. Stout and S.S. Hecker, *Material Behavior under High Stress and Ultrahigh Loading Rates,* Plenum Press, 1983, p 39-60
117. Y. Tozawa, "Flow Stress of Materials for Cold Forging under Forming Conditions," presented at 20th Plenary Meeting of ICFG, Warsaw, 1987
118. Z. Marciniak and A. Konieczny, in *Advanced Technology of Plasticity 1987,* K. Lange, Ed., Springer, Berlin, 1987, p 17-22